ACS Infectious Diseases

pubs.acs.org/journal/aidcbc

Article

Two-Way Regulation of MmpL3 Expression Identifies and Validates Inhibitors of MmpL3 Function in *Mycobacterium tuberculosis*

Shipra Grover,* Curtis A. Engelhart, Esther Pérez-Herrán, Wei Li, Katherine A. Abrahams, Kadamba Papavinasasundaram, James M. Bean, Christopher M. Sassetti, Alfonso Mendoza-Losana, Gurdyal S. Besra, Mary Jackson, and Dirk Schnappinger*

Cite This: *ACS Infect. Dis.* 2021, 7, 141−152

Read Online

ACCESS | Metrics & More | Article Recommendations | Supporting Information

ABSTRACT: MmpL3, an essential mycolate transporter in the inner membrane of *Mycobacterium tuberculosis* (*Mtb*), has been identified as a target of multiple, chemically diverse antitubercular drugs. However, several of these molecules seem to have secondary targets and inhibit bacterial growth by more than one mechanism. Here, we describe a cell-based assay that utilizes two-way regulation of MmpL3 expression to readily identify MmpL3-specific inhibitors. We successfully used this assay to identify a novel guanidine-based MmpL3 inhibitor from a library of 220 compounds that inhibit growth of *Mtb* by largely unknown mechanisms. We furthermore identified inhibitors of cytochrome bc_1-aa_3 oxidase as one class of off-target hits in whole-cell screens for MmpL3 inhibitors and report a novel sulfanylacetamide as a potential QcrB inhibitor.

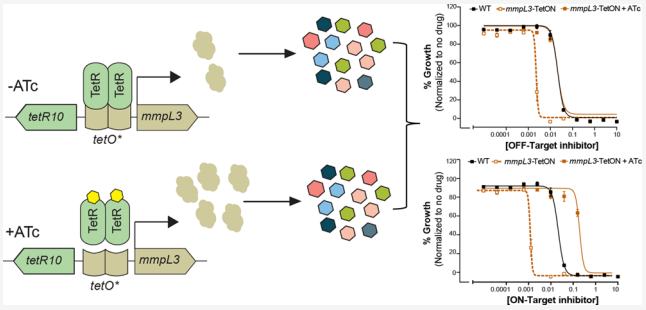

KEYWORDS: *targeted whole-cell screen, mycolic acids, antibiotics, molecular genetics, drug discovery, respiration*

Mycobacterium tuberculosis (*Mtb*), etiologic agent of tuberculosis (TB), is the leading cause of adult mortality due to a single infectious agent in both healthy and HIV-infected individuals. In 2019, the World Health Organization (WHO) estimated a total of 1.7 billion people to be infected with *Mtb* and at risk of developing the disease.[1] The preferred treatment for drug-susceptible TB requires at least four drugs with toxic side effects, administered routinely for a minimum of two months during the intensive phase and at least two drugs during the continuation phase of four months.[1] This leads to poor compliance, which accelerates the emergence of drug-resistance, and causes relapse of disease.[2,3] Reducing the global TB epidemic necessitates development of new therapeutics to shorten the duration of treatment and to be effective against the drug-resistant forms of infection.

To facilitate TB drug discovery efforts, whole-cell screens (WCS) against *Mtb* have identified the highest number of novel pharmacophores with potent antimycobacterial activity.[4,5] Interestingly, multiple chemical entities discovered using this approach primarily target MmpL3, an essential lipid transporter in mycobacteria.[6−14] A member of the resistance nodulation and division (RND) superfamily of transporters, MmpL3 facilitates transport of trehalose monomycolate (TMM) into the periplasmic space where it is modified and assembled into the outer layer of the mycobacterial cell envelope.[15−17] Chemical and genetic inhibition of MmpL3 leads to a sharp decline in mycolate transport, bacterial growth, and viability, both *in vitro* and in the mouse model of TB, rendering it a significant target of therapeutic interest.[6−10,18−21] Anti-MmpL3 pharmacophores, including adamantyl ureas,[9] pyrroles,[7] indolecarboxamides,[20] diamines,[6,22] tetrahydropyrazolopyrimidines (THPPs), and spirocycles (Spiros),[8,23] are active against drug-resistant strains of *Mtb*. In addition, several of these scaffolds synergize with existing antitubercular drugs, for example, rifampicin, suggesting that inhibition of MmpL3 could shorten TB treatment.[8,10,24−29] Among these pharmacophores, the diamine SQ109 has successfully completed phase 2b-3 of clinical trials[30,31] and others such as indolecarboxamides, pyrroles, and THPPs exhibit favorable pharmacokinetic profiles and efficacy in murine models of infection.[7,8,10]

To date, identification and characterization of MmpL3 inhibitors relies on integration of cell-based screenings of chemical libraries with genetic techniques, such as isolating resistant mutants and performing cross-inhibition experiments, followed by chemical-radiolabeling to assess TMM levels to

Received: September 28, 2020
Published: December 15, 2020

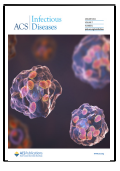

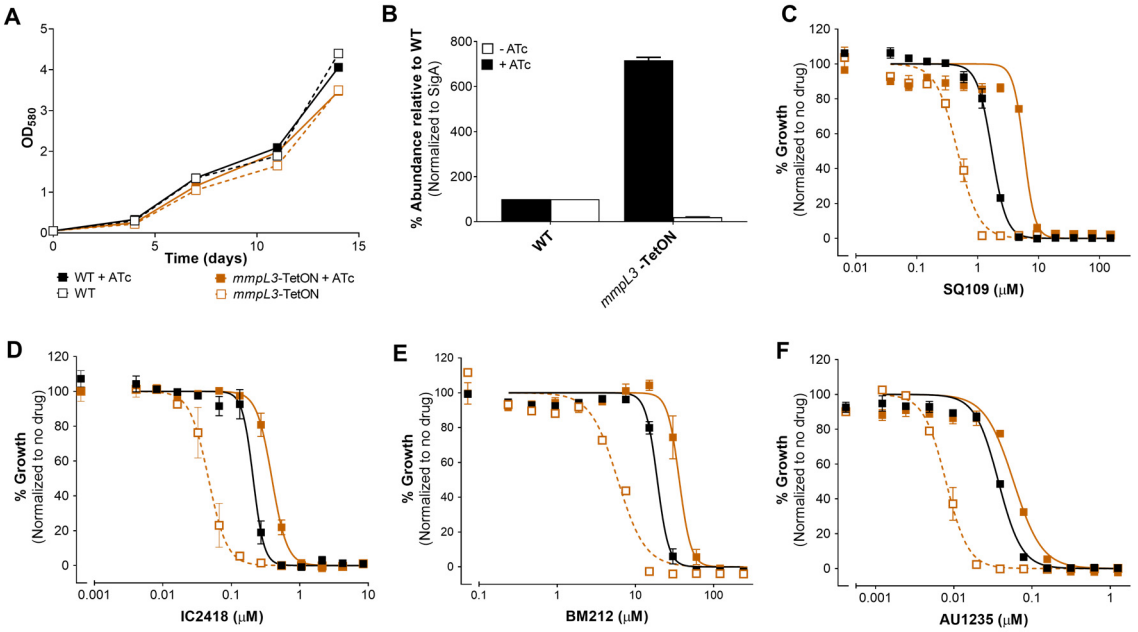

Figure 1. Consequences of two-way regulation of *mmpL3* on growth, protein expression, and susceptibility to on-target MmpL3 inhibitors. (A) Growth and (B) protein levels of MmpL3 in *mmpL3*-TetON in the absence and presence of inducer ATc. (C−F) Dose−response profiles of MmpL3 inhibitors against *mmpL3*-TetON (orange) in the absence (open, dashed) and presence (closed, solid) of ATc (500 ng/mL) vs WT (black). Data are representative of three experiments; values are averages of two technical replicates and error bars represent the standard error (SE) of the mean. See also Table S2.

identify the target. While informative, most of these methods are laborious, compound-intensive, and difficult to implement in a high-throughput format, hence limiting their utility. The need to simplify identification of MmpL3 inhibitors was recently addressed by an elegant study, which utilized a pool of 24 unique *mmpL3* mutants. Each mutant caused resistance against a subset of the known MmpL3 inhibitors. This increases screening efficiency significantly, but only for compounds susceptible to already known resistance mutations.[32] Furthermore, a cohort of MmpL3 inhibitors, including THPPs, seems to impede bacterial growth either by inhibition of multiple targets[23,33] or by general mechanisms, such as dissipation of proton motive force (PMF), necessary for substrate translocation, rendering it difficult to distinguish between on- and off-target inhibitors of this target.[34,35]

Here, we report a whole-cell assay encompassing a transcriptionally regulated strain of MmpL3, *mmpL3*-TetON, with two-way regulation of protein expression in *Mtb* to identify and segregate on-target inhibitors. We first characterized the consequences of regulating MmpL3 on growth, membrane permeability, and susceptibility to known MmpL3 inhibitors and existing antibiotics. Next, we performed a cell-based phenotypic screen utilizing the *mmpL3*-TetON strain against 220 compounds comprising the GSK-Tres Cantos antimycobacterial set (TB-set) to identify new inhibitors in addition to validating the previously characterized scaffolds. Furthermore, using an *Mtb* knockout of cytochrome *bd* oxidase, we could discern inhibitors of cytochrome bc_1-aa_3 oxidase as most likely to indirectly interfere with MmpL3 activity. This approach identified a sulfanylacetamide as a probable cytochrome bc_1-aa_3 oxidase inhibitor. Finally, we established a guanidine-based compound, CCI7967, as an on-target inhibitor of MmpL3. Our work highlights the value of target-based phenotypic screens to identify novel antimycobacterial inhibitors. These assays have significant utility in facilitating prompt identification of new lead molecules and target-driven optimization of analogues of more advanced scaffolds that inhibit MmpL3 activity in a cellular context.

RESULTS

Consequences of Two-Way Regulation of MmpL3 on Growth, Protein Expression, and Susceptibility to On-Target MmpL3 Inhibitors. We constructed a transcriptionally regulated MmpL3 strain, *mmpL3*-TetON, as previously described for *trxB2*.[36] The *mmpL3*-TetON strain and wild-type H37Rv (WT) grew with similar kinetics in either the absence or presence of 500 ng/mL of anhydrotetracycline (ATc) (Figure 1A). MmpL3 expression was quantified by LC-MS/MS using MmpL3-specific peptides and normalized to the essential sigma factor SigA of RNAP, which is constitutively expressed during growth and commonly used as reference in expression studies.[37] Compared to WT, *mmpL3*-TetON with ATc displayed a 717% increase in MmpL3 expression while its cultivation in ATc-free media resulted in an 80% decrease (Figure 1B). Therefore, *mmpL3*-TetON provides two-way regulation, overexpression, and under-expression of MmpL3, without compromising the growth of *Mtb*.

Next, we examined the susceptibility of *mmpL3*-TetON toward the clinical candidate SQ109 (diamine) (Figure 1C) and three other compounds, IC2418 (indolecarboxamide) (Figure 1D), BM212 (pyrrole) (Figure 1E), and AU1235 (adamantyl urea) (Figure 1F), that reduce the growth of *Mtb via* inhibition of MmpL3. All four compounds were more potent against *mmpL3*-TetON than WT when both strains were grown without ATc and less potent against *mmpL3*-TetON when grown with ATc (Figure 1C−F, Table S1). The dose−response profiles thus showed a bidirectional shift in IC_{50} in response to MmpL3 regulation, suggesting that *mmpL3*-TetON could be used to identify inhibitors of MmpL3.

https://dx.doi.org/10.1021/acsinfecdis.0c00675
ACS Infect. Dis. 2021, 7, 141−152

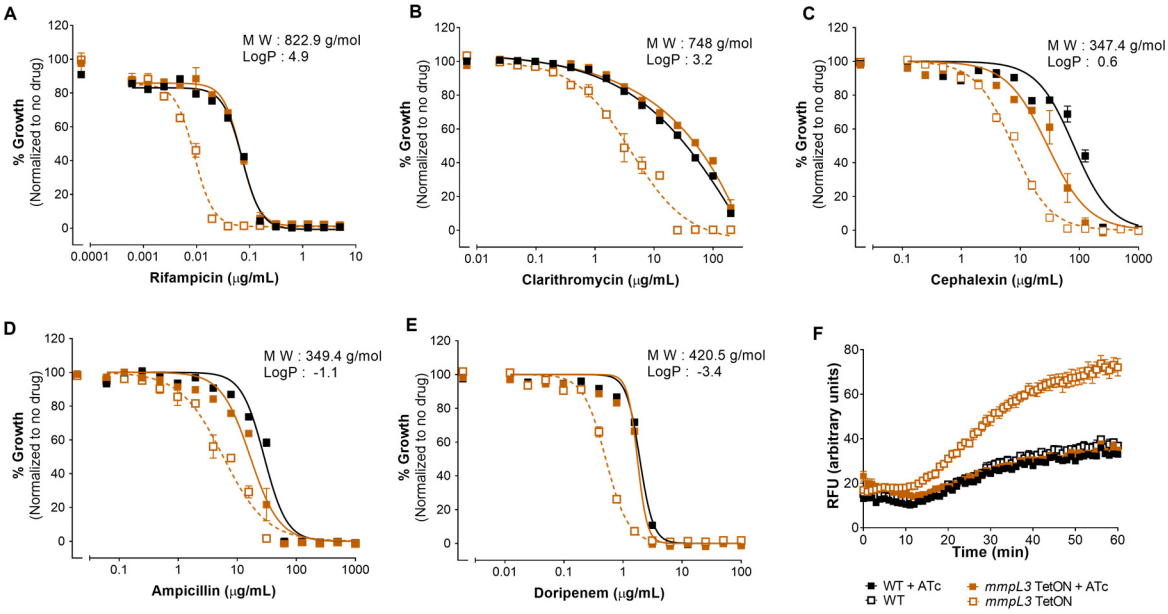

Figure 2. Silencing of MmpL3 expression alters cell envelope permeability to specific off-target inhibitors. (A–E) Dose–response profiles of *mmpL3*-TetON (orange) in the absence (open, dashed) and presence (closed, solid) of ATc (500 ng/mL) against high molecular weight antibiotics (A) rifampicin and (B) clarithromycin; and to different classes of (C–E) β-lactams. Data are representative of three experiments; values are averages of three technical replicates and error bars represent the SE of the mean. (F) Impact of MmpL3 depletion on accumulation of EtBr. The strains were incubated with 8 μg/mL of EtBr in PBS supplemented with 0.05% Tyloxapol and 0.4% Glucose. Reads were collected every minute until 60 min at 37 °C. See also Figure S2.

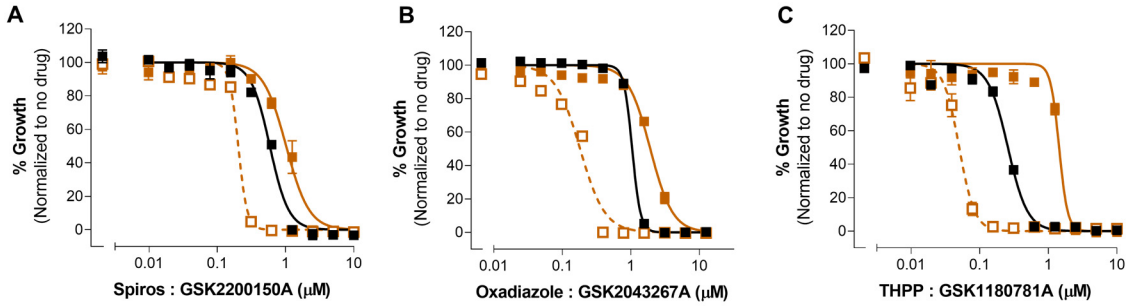

Figure 3. Susceptibility profile of *mmpL3*-TetON against the on-target hits. (A–C) Impact of selected screening hits on *mmpL3*-TetON (orange) and WT (black). For *mmpL3*-TetON, measurements were performed without (open squares, dotted lines) and with (closed squares, solid lines) ATc (500 ng/mL). Data are representative of three biological and two technical replicates. See also Figure S3 and Table S1.

Compounds Indirectly Affected by MmpL3 Display a Unidirectional Shift against *mmpL3*-TetON. Next, we investigated the potency of chemically and mechanistically diverse antibiotics toward WT and *mmpL3*-TetON. The potency of 22 antibiotics (Figure S1) was similar against *mmpL3*-TetON and WT when grown in the absence of ATc. This included fluoroquinolones, such as ciprofloxacin, and mycolate synthesis inhibitors, such as isoniazid, that behaved as previously reported.[38] However, when cultivated without ATc, *mmpL3*-TetON was hyper-sensitized to rifampicin (Figure 2A), clarithromycin (Figure 2B), erythromycin, fidaxomicin (Figure S2), and fusidic acid (Figure S2). MmpL3 depletion also increased activity of different β-lactams, cephalexin (Figure 2C), cefadroxil, cefdinir (Figure S2), ampicillin (Figure 2D), carbenicillin (Figure S2), doripenem (Figure 2E), imipenem, and faropenem (Figure S2). In contrast to the direct inhibitors of MmpL3 activity, the potency of these compounds did not shift for *mmpL3*-TetON when grown in the presence of ATc. A unidirectional MIC shift thus distinguished compounds that were affected indirectly by a reduction in MmpL3 expression from direct MmpL3 inhibitors that had displayed a bidirectional MIC shift.

MmpL3 mediates the transport of TMM, which suggests that reducing its expression could alter the fluidity of the mycobacterial cell envelope and modify its permeability.[39,40] To test this, we performed an ethidium bromide (EtBr)-based uptake assay[41] for WT and *mmpL3*-TetON. When grown with ATc, EtBr uptake of *mmpL3*-TetON was similar to that of WT (Figure 2F). However, when grown without ATc, *mmpL3*-TetON exhibited a 3-fold increase in EtBr uptake relative to the WT. The increased susceptibility that resulted from under-expression of MmpL3 for growth inhibition by mechanistically diverse drugs such as rifampicin, clarithromycin, erythromycin, and fidaxomicin, which are all large (>500 Da) and hydrophobic (log P > 2.5), might thus be due to differences in drug uptake. Conversely, the increased potency of hydrophilic antibiotics such as β-lactams could be governed by defects in outer membrane permeability or by mechanisms not entirely understood.

https://dx.doi.org/10.1021/acsinfecdis.0c00675
ACS Infect. Dis. 2021, 7, 141–152

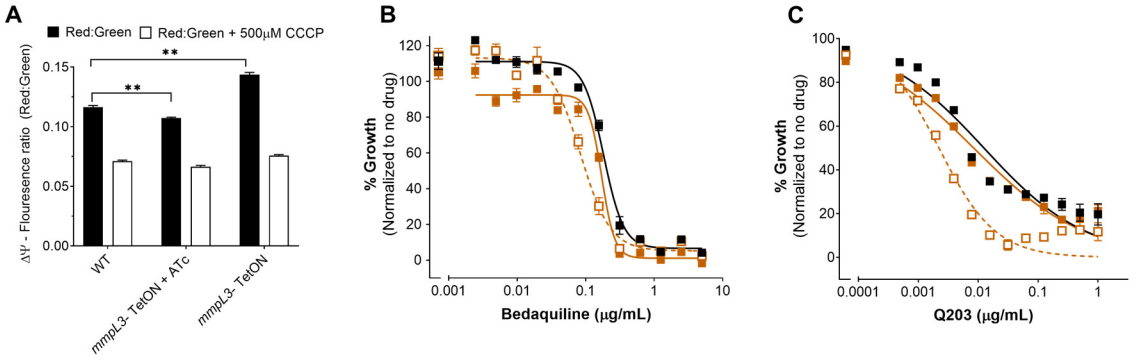

Figure 4. Impact of MmpL3 expression on membrane potential and the activity of ETC inhibitors. (A) Effect on membrane potential (ΔΨ). $DiOC_2(3)$ accumulation was assessed in *mmpL3*-TetON in the presence and absence of ATc (500 ng/mL) before (solid) and after (hollow) exposure to 500 μM CCCP for 30 min at 37 °C. Student's unpaired *t* test ($p < 0.01$) was performed to determine statistical significance of differences between the mutant groups denoted with **. (B,C) Dose−response profile of *mmpL3*-TetON (orange) in absence (open, dashed) and presence (closed, solid) of ATc (500 ng/mL) against (B) the ATP synthase inhibitor bedaquiline and (C) the cytochrome bc_1-aa_3 inhibitor Q203. Data are representative of three experiments; values are averages of three technical replicates and error bars represent the SE of the mean.

Targeted Whole-Cell Phenotypic Screen to Identify Inhibitors of MmpL3 Function. To investigate the utility of two-way regulation in identifying scaffolds that inhibit mycolate transport, we evaluated *mmpL3*-TetON and WT against a library of 220 compounds in the GSK Tb-set.[5,42] Bacteria were grown without ATc and subjected to up to 10 doses of the compounds with concentrations ranging between 100 and 0.005 μM including 1% DMSO (negative control) and 1 μg/mL rifampicin (positive control). The screen presented a Z′ value >0.8. Compounds that inhibited the growth of WT by at least 30% at the highest concentration were re-evaluated against WT and *mmpL3*-TetON with and without ATc. This identified 26 hits (Table S1, Figure S3), which were then assessed for changes in IC_{50}. All 26 compounds displayed a decrease in IC_{50} against the *mmpL3*-TetON without ATc. Of these, 12 compounds displayed >1.5-fold increase in IC_{50} against *mmpL3*-TetON with ATc, which were categorized as on-target hits. Six of the on-target hits (denoted with * in Table S1) were excluded from subsequent analyses due to lack of availability and poor solubility. The remaining hits were distributed in three scaffolds including Spiros (Figure 3A and Table S1),[8] oxadiazoles (Figure 3B and Table S1),[43] and THPPs (Figure 3C and Table S1).[8] Interestingly, we observed inconsistency in phenotype for members of two scaffolds, Spiros (SB-354364, Table S1) and cycloalkanes (GSK2783100A*, Table S1),[44] as neither confirmed to target MmpL3. The singleton hydroxypiperidine (GSK1985270A, Table S1) that seems to target MmpL3 in both *Mtb* and *Mycobacterium abscessus* (*Mab*)[45,46] displayed no change in potency against the *mmpL3*-TetON with ATc.

The THPPs identified herein accounted for 42% of the on-target hits with all presenting a bidirectional shift of the highest magnitude of the scaffolds tested. Mutations conferring THPP resistance also map to one target, MmpL3,[34,47] and THPPs bind MmpL3,[34] rendering it a pivotal target. However, THPPs also interact with an enoyl-coenzyme A hydratase, EchA6, to suppress mycolic acid synthesis, deeming it a second target.[23] We confirmed the stereospecificity of new THPPs for EchA6 (Figure S4) in an intrinsic tryptophan fluorescence binding assay against the purified *Mtb*-EchA6.[23] As expected, the compounds bound with a K_D ranging from 0.62−6.86 μM, similar to the previously reported THPPs, GSK366A (K_D = 1.01 ± 0.38 μM) and GSK951A (K_D = 0.64 ± 0.16 μM) further supporting EchA6 as a second target.

Partial Expression of MmpL3 Identifies Inhibitors of Cytochrome bc_1-aa_3. The crystal structure of MmpL3 defined a dedicated H^+ translocation channel in the protein that drives the translocation of TMM across to the periplasmic space.[35] Co-crystal structures and molecular docking studies suggest that most MmpL3 inhibitors reduce TMM translocation by binding and blocking the H^+ relay channel.[35] This motivated us to further explore the relationship between membrane polarization and MmpL3 activity. We first analyzed the impact of MmpL3 expression on the membrane potential (ΔΨ) using the ΔΨ-sensitive cyanine dye $DiOC_2(3)$.[48] Red fluorescence of $DiOC_2(3)$ indicates an intact membrane potential, whereas its dissipation, for example, by treatment with the PMF uncoupler CCCP, is accompanied by a shift from red to green fluorescence. $DiOC_2(3)$ fluorescence of *mmpL3*-TetON grown with ATc was similar to that of WT but red-shifted when grown without ATc. This suggested that MmpL3 under-expression led to an increase in ΔΨ, as reported previously,[32,34] while its overexpression led to a small decrease in ΔΨ (Figure 4A).

RND transporters rely on PMF and PMF-disrupters, such as CCCP, can inhibit the RND transport activity.[33] Molecules that affect the electron transport chain (ETC), which is responsible for generation and maintenance of PMF, could thus represent one class of inhibitors whose potency increases upon MmpL3 under-expression without interacting with MmpL3 directly. We tested the impact of MmpL3 under-expression on ETC inhibitors with Q203[49] and bedaquiline,[50,51] that inhibit *Mtb*'s cytochrome bc_1-aa_3 oxidase and ATP synthase, respectively. Silencing of MmpL3 only had a modest effect on bedaquiline but enhanced the activity of Q203 (Figure 4B,C), which identified inhibitors of cytochrome bc_1-aa_3 oxidase as potential off-target hits.

Furthermore, the hits we classified as indirect inhibitors of MmpL3 included two scaffolds, imidazopyridine amine (IPA) and quinolone (QoA), reported to target cytochrome bc_1-aa_3 oxidase.[52,53] The cytochrome bc_1-aa_3 oxidase functions in conjunction with cytochrome *bd* oxidase and inactivation of both leads to rapid killing of *Mtb*.[54] Accordingly, inhibitors of cytochrome bc_1-aa_3 oxidase are more potent against a knockout of cytochrome *bd* oxidase (Δ*cydABDC*) than WT.[55] To

https://dx.doi.org/10.1021/acsinfecdis.0c00675
ACS Infect. Dis. 2021, 7, 141−152

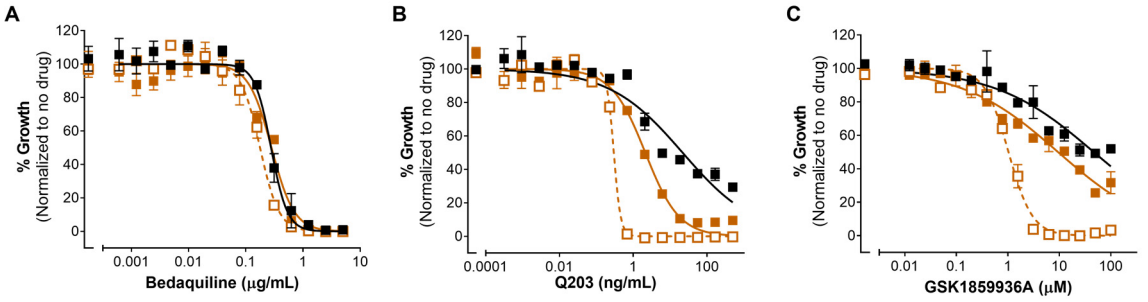

Figure 5. Partial expression of MmpL3 identifies a sulfanylacetamide as an inhibitor of cytochrome bc_1-aa_3 oxidase. Dose−responses profiles of the cytochrome *bd* oxidase knockout (orange, open, dashed) and complemented strain (orange, closed, solid) vs WT (black) against (A) bedaquiline, (B) Q203, and (C) GSK1859936A. Data are representative of three experiments; values are averages of three technical replicates and error bars represent the SE of the mean.

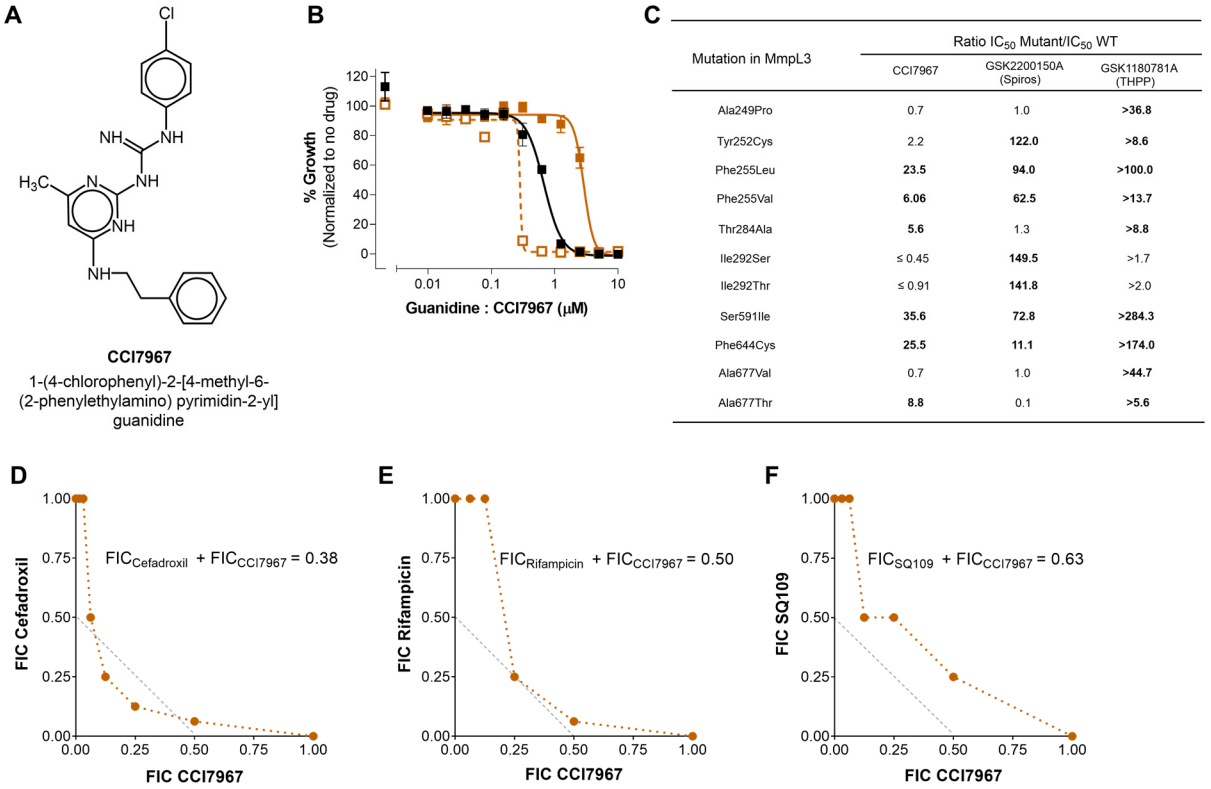

Figure 6. CCI7967 is an MmpL3 inhibitor. (A) Structure of CCI7967. (B) Dose−response profile of *mmpL3*-TetON (orange) in the absence (open, dashed) and presence (closed, solid) of ATc (500 ng/mL). (C) Cross-resistance depicted as the ratio of IC_{50} between the mutant and WT for different mutations in MmpL3 for CCI7967, GSK2200150A (Spiros), and GSK1180781A (THPP). (D−F) Isobolograms of CCI7967 tested in combination with (D) β-lactam, cefadroxil; (E) RNA polymerase inhibitor, rifampicin; and (F) MmpL3 inhibitor, SQ109.

investigate whether the remaining off-target scaffolds included additional cytochrome bc_1-aa_3 oxidase inhibitors, we measured their activity against Δ*cydABDC*. In concordance with previous results,[55] the MIC of bedaquiline against the Δ*cydABDC* remained relatively unchanged (Figure 5A) whereas the MIC of Q203 decreased substantially (Figure 5B). A sulfanylacetamide, GSK1859936A, demonstrated augmented potency akin to Q203 (Figure 5C), suggesting cytochrome bc_1-aa_3 oxidase as the target of GSK1859936A. The potency of scaffolds that inhibit MmpL3 directly remained largely unchanged against the knockout of cytochrome *bd* oxidase (Figure S5). Deletion of *cydABDC* too did not change the MIC of thienopyrimidine amines (TPAs), aminothiazoles, or pyridine-2-carboxamides, indicating an alternative mode of growth inhibition by these scaffolds (Figure S6). In contrast, IPAs and QoA were, as expected, more potent against Δ*cydABDC*, which further validates cytochrome bc_1-aa_3 as a target for these scaffolds (Figure S7).

Guanidine-Based CCI7967 Is an MmpL3 Inhibitor. Our screen classified CCI7967, 1-(4-Chlorophenyl)-2-[4-methyl-6-(2-phenylethylamino) pyrimidin-2-yl] guanidine (Figure 6A), as a direct inhibitor of MmpL3. Its IC_{50} was 2.4-fold lower against *mmpL3*-TetON than WT in the absence of ATc and 4.3-fold higher against *mmpL3*-TetON than WT in the presence of ATc (Figure 6B and Table S1). To gain further insight into its target, we isolated spontaneous mutants to CCI7967. Approximately 9×10^{-7} of the bacteria plated grew on agar plates containing CCI7967 at a concentration of 4-fold the MIC. This suggests that the frequency of resistance against CCI7967 is similar to what has been observed for other

https://dx.doi.org/10.1021/acsinfecdis.0c00675
ACS Infect. Dis. 2021, 7, 141−152

MmpL3 inhibitors, for which resistance frequencies range between 10^{-7} and 10^{-8}.[7−9,20] Whole-genome sequencing identified two SNPs, T284A and A677T, in MmpL3 that imparted a 5- to 8-fold change in IC_{50} against CCI7967 (Figure 6C). We also assessed the cross-inhibitory activity of CCI7967 toward previously reported MmpL3 resistant mutants[8] isolated against Spiros and THPP compounds to confirm MmpL3 as the target (Figure 6C). The fold changes in IC_{50} were variable, with the S591I SNP imparting up to 35-fold resistance to CCI7967. This substitution was previously found to confer pan-resistance to several MmpL3 inhibitors.[32]

Previously, a synergistic association of SQ109 with rifampicin and β-lactams was assigned to be a signature of MmpL3 inhibitors.[19,28] On this basis, we determined if CCI7967 synergizes with rifampicin and β-lactams. The drug combinations were assessed in a checkerboard assay format and the isobolograms were generated by plotting the FIC_A vs FIC_B (Figure 6D−F). As expected, the combination of CCI7967 with cefadroxil (Figure 6C) and rifampicin (Figure 6D) presented FICI $\leq$ 0.5 with a convex, inward-bowing isobologram indicative of synergism while no significant interaction of CCI7967 with SQ109 (Figure 6F) was evident, suggestive of a shared target for the two inhibitors. Collectively, these data confirm CCI7967 to be an MmpL3 inhibitor.

DISCUSSION

MmpL3 is essential to the integrity of the mycobacterial cell envelope which contributes to the intrinsic resistance of mycobacteria to antimicrobials. To facilitate discovery and development of MmpL3 inhibitors, we developed a simple and robust assay that utilized two-way regulation of MmpL3 expression to select for target-specific compounds. That under-expression can be exploited to identify small-molecules that inhibit a target of interest in *Mtb* has been demonstrated previously.[56−58] However, the two-way system described herein greatly facilitates to distinguish molecules that engage the target of interest directly from those that are potentiated due to indirect effects. Easy to implement in HTS format, when applied against the GSK Tb-set, this methodology validated several of the previously identified MmpL3 inhibitors with a few exceptions, notably, SB-354364 (Spiros), and a closely related compound, GSK1985270A (hydroxypiperidine) (Figure S3).[8,45,46] The two cycloalkanes (GSK2623870A* and GSK2783100A*) also displayed differences in their dependence on MmpL3 expression. Since high vulnerability of MmpL3 can potentially mask secondary effects or targets of the selected hits, it is plausible that the variation observed in these cases could be attributed to scaffolds having secondary targets, as is evident for THPPs[23] and for a few analogues of Spiros.[59] The likelihood of a compound from a scaffold presenting a bidirectional shift in our assay relies on its affinity toward MmpL3, and when structurally modified could alter this bias in favor of the secondary target rendering it difficult to be identified as an on-target inhibitor. An example of this was seen for THPPs, wherein a point mutation, W133A in EchA6, increased the *in vitro* MIC and effective dose in mice.[23] Interestingly, THPP-resistance conferring mutations mapped to the H^+ translocation domains of MmpL3,[8,35] similar to all other MmpL3 inhibitors identified to date, suggesting that increased efflux is not the mechanism of resistance.[35] Therefore, it is likely that MmpL3's vulnerability coupled with its ability to bind diverse scaffolds and a range of cellular ligands[47] could render it as a sink for most compounds consequently limiting their access to other target(s).

Molecules whose potency increased in response to MmpL3 depletion but did not decrease after MmpL3 overexpression were classified as off-target hits. For several hits, including TPAs (GSK237561A and GSK153890A), aminothiazoles (GSK690382A and GSK445886A),[59,60] and a pyrdine-2-carboxamide (GSK1750922A), this classification was supported by cross-resistance measurements as IC_{50} values were only affected 0.4- to 5-fold by known resistance mutations in *mmpL3* (Table S2). Inhibitors of cytochrome bc_1-aa_3 oxidase, including IPA,[52] QoA,[53] piperazine,[61] and a novel sulfanylacetamide (GSK1859936A), were frequent off-target hits. Enrichment of these inhibitors in our screen might be related to the repression of genes linked to energy metabolism that has been observed in response to inactivation of MmpL3.[18] The mechanisms underlying other off-target inhibitors likely include increased target access, as seen for rifampicin and β-lactams, and, potentially, inhibition of other steps in or linked to mycolic acid synthesis or transport, a possibility that requires further exploration.

Our assay also identified a novel guanidine, CCI7967, as an MmpL3 inhibitor with the characteristic bidirectional shift. Its on-target activity was further evidenced by resistance mutants against the compound yielding mutations in MmpL3 and cross-resistance to other SNPs in the transporter. These three approaches—under-expression, overexpression, and identification of resistance mutations—helped discern CCI7967 as an on-target inhibitor, which can be confirmed in future studies by monitoring TMM accumulation, or direct interaction with MmpL3.[34] Furthermore, the interaction of CCI7967, similar to previously reported MmpL3 inhibitors,[27] was synergistic with rifampicin and cefadroxil but additive with SQ109. The cell-based assays we developed can thus be used to screen for new small molecules that inhibit the growth of *Mtb* in an MmpL3-dependent manner and subsequently distinguish those molecules that are likely to target MmpL3 directly from those whose potency is only indirectly affected by MmpL3.

Aside *Mtb*, MmpL3 is emerging as an important drug-target in other rapidly growing pathogenic nontuberculosis mycobacteria such as *Mab*.[46,62−69] An arising opportunist, *Mab* is inherently resistant to several of the existing antibiotics which drastically limits the treatment options for infection.[70,71] At present, the discernment of new MmpL3 inhibitors with activity against *Mab* relies on phenotypic screens[46,63,66,69] and cross-species inhibition experiments.[67] Since *Mab* and *Mtb* are closely related, the two way system described herein could subsequently be adapted in *Mab* to supplement the ongoing drug discovery efforts.

METHODS

Construction of *mmpL3*-TetON. We first generated an *mmpL3* merodiploid by integrating the constitutive *mmpL3* expression plasmid pGMCS-Ptb38-*mmpL3* ($Strep^R$) into the attachment site of the phage L5 (attL5) of *M. tuberculosis* H37Rv. Next, the wild-type (WT) copy of *mmpL3* was inactivated by homologous recombination using the knockout construct previously used to generate *mmpL3*-DUC.[19] Deletion of the WT copy of *mmpL3* resulted in H37Rv pGMCS-Ptb38-*mmpL3*, in which the only copy of *mmpL3* is expressed from the attL5 site. The *mmpL3*-TetON was generated by transforming H37Rv pGMCS-Ptb38-*mmpL3* with the *mmpL3*-TetON plasmid pGMCZ-0X-T10M-P606-

https://dx.doi.org/10.1021/acsinfecdis.0c00675
ACS Infect. Dis. 2021, 7, 141−152

5C-mmpL3 and screening for colonies that were resistant to zeocin and susceptible to streptomycin. Streptomycin sensitivity assured replacement of the constitutive pGMCS-Ptb38-*mmpL3* by pGMCZ-0X-T10M-P606-*5C-mmpL3*. Plasmid replacement and regulation of MmpL3 expression was further confirmed by protein quantification and phenotypic assays.

Plasmids, Bacterial Strains, and General Procedures. The WT and its derivatives were grown in Middlebrook 7H9 medium supplemented with 0.2% (v/v) glycerol, 0.05% (v/v) tyloxapol, 0.5% (w/v) Bovine Serum Albumin (BSA, Roche), 0.2% (w/v) dextrose, and 0.085% (w/v) NaCl (ADN), or on Middlebrook 7H10 agar supplemented with 10% (v/v) oleic acid-albumin-dextrose-catalase (OADC; BD, Difco) and 0.5% (v/v) glycerol at 37 °C unless otherwise specified. Hygromycin (Roche), streptomycin (Sigma-Aldrich), kanamycin (Sigma-Aldrich), zeocin (Thermo Fisher) and anhydrotetracycline (ATc, Sigma-Aldrich) were used at a concentration of 50, 25, 25, and 25 μg/mL, and 500 ng/mL, respectively. For experiments with the regulated strain, the wild-type and *mmpL3*-TetON strains were cultured until mid log phase (OD_{580} 0.6−0.8) in the presence of 500 ng/mL ATc at 37 °C. To trigger regulation, cells were harvested, washed, and resuspended to an $OD_{580} \approx 0.05$ in Middlebrook 7H9−ADN supplemented with and without ATc and incubated for up to seven generations (doubling time approximately 24 h) at 37 °C. Protein levels were further altered by rediluting cultures to an $OD_{580} \approx 0.01$ and incubated for a minimum of five generations (doubling time approximately 24 h) under the same growth conditions as mentioned above to perform subsequent experiments. The knockout of cytochrome *bd* oxidase (Δ*cydABDC*) and complement was grown as previously described.[55]

Identification and Quantitation of MmpL3 by LC-MS/MS. The transcriptionally regulated strain of *mmpL3* and the parental H37Rv were initially grown until mid log phase in the presence of 500 ng/mL ATc at 37 °C. To trigger regulation, cells were harvested, washed, and resuspended to an $OD_{580} \approx 0.05$ in Middlebrook 7H9−ADN supplemented with and without ATc and incubated for up to seven generations (doubling time approximately 24 h) at 37 °C. Protein levels were further altered by rediluting cultures to an $OD_{580} \approx 0.01$ in same growth conditions and incubated for a minimum of five generations (doubling time approximately 24 h). Bacterial lysates for targeted proteomics were prepared using a previously published protocol.[72] Briefly, protein extracts were prepared from 30 mL cultures by bead beating pellets with Lysing Matrix Beads (MP Biomedical) in PBS supplemented with 2% SDS and cOmplete EDTA−protease-free inhibitor cocktail (Roche). Lysate protein concentrations were determined using a BCA-protein assay kit (Pierce, Thermo Scientific). Lysates corresponding to 50 μg total protein were subjected to electrophoresis for a short distance through a 4−20% mini PROTEAN TGX gradient gel (Bio-Rad) under denaturing conditions for approximately 2 cm into the gel. After staining with Novex Colloidal Blue staining kit (ThermoFisher Scientific), and destaining with water, the gel pieces containing almost all of the proteins were excised out, processed for trypsin digestion and subjected to LC/MS/MS for Parallel Reaction Monitoring (PRM) analysis similar to that published previously.[73] Briefly, a 3.0 μL aliquot of trypsin-digested sample was directly injected onto a custom packed 2 cm × 100 μm C18 Magic 5 μm particle trap column. Peptides were then eluted and sprayed from a custom packed emitter (75 μm × 25 cm C18 Magic 3 μm particle) with a linear gradient from 95% solvent A (0.1% formic acid in water) to 35% solvent B (0.1% formic acid in Acetonitrile) in 90 min at a flow rate of 300 nanoliters per minute on a Waters Nano Acquity UPLC system. Data dependent acquisitions were performed on a Q Exactive mass spectrometer (Thermo Scientific) according to an experiment where full MS scans from 300 to 1750 m/z were acquired at a resolution of 70 000 followed by 10 MS/MS scans acquired under Higher-energy C-trap dissociation (HCD) fragmentation at a resolution of 17 500 with an isolation width of 1.6 Da. Six tryptic peptides of MmpL3 (residues 97−113 FQQDHPDQVLGWAGYLR, 163−182 LAGLQPVAEALTGTIATDQR, 510−523 VLQNGLINPADASK, 744−755 IGLGEIHLPDER, 801−829 SSPASSPELTPALEATAAPAAPSGASTTR, and 882−900 STDAAGDPAEPTAALPIIR) and four tryptic peptides of SigA (238−251 VALLNAEEEVELAK, 410−418 VLEIQQYAR, 479−487 FGLTDGQPR, and 488−500 TLDEIGQVYGVTR; all annotations as per http://tuberculist.epfl.ch) were selected to monitor the protein abundance in the samples. Three fragment ion intensities that generated the most robust signals were extracted from each peptide and summed to determine the peptide abundance. Quantification of targeted peptides was accomplished through the Skyline software (University of Washington). The average of peptide abundance from two technical replicates were analyzed for each sample. The relative level of MmpL3 was calculated by normalizing the total transition area of each of the six MmpL3 peptides to that of each of the four SigA peptides. Data represent the mean ± SE obtained from the normalized values.

Drug Susceptibility Assays. The compounds used in this study were sourced from Sigma-Aldrich and GlaxoSmithKline (GSK). Bedaquiline, Q203, Pretomanid (PA-824), and BM212 were procured from MedChemExpress. IC2418 and AU1235 were sourced from Mary Jackson, Colorado State University. Compounds had a purity of >98%, as determined by HPLC and ^{1}H NMR analysis and were dissolved and stored in dimethyl sulfoxide for use. Susceptibility assays were performed in black/clear, flat-bottom 384-well microplates (Grenier Bio-One) by dispensing nanoliter volume of drugs into 2-fold dilutions with a minimum of 10 doses per drug using an automated drug dispenser (D300e Digital Dispenser, HP). The DMSO concentrations in all wells were normalized to 1%, controls included DMSO at 1% and rifampicin at 1 μg/mL for 100% growth and 100% inhibition, respectively. Mid log phase cultures were diluted to an optical density (OD_{580}) ≈ 0.01 in fresh 7H9−ADN media and wells were seeded with 50 μL of bacteria. Inoculated plates were stacked, covered with a sterile lid, wrapped with aluminum foil to prevent evaporation, and allowed to incubate at 37 °C, 5% CO_2 at 80% relative humidity for up to 10 days. Growth measurements were recorded at OD_{580} using a spectrophotometer (SpectraMax M5 or M2e). IC_{50} values were determined using the variable-slope four-parameter nonlinear least-squares regression model in GraphPad Prism software package (version 8).

To determine the MIC of the compound on solid media, 7H10 agar supplemented with 10% OADC and 0.5% glycerol was used to prepare 2-fold serial dilutions of CCI7967 at concentrations ranging from 100−0.097 μM. Mid log phase cultures were grown to an OD_{580} of 0.8−1 and diluted to a final concentration of 10^6 CFU/mL and 10 μL was spotted onto each dilution. The plates were incubated at 37 °C for up

https://dx.doi.org/10.1021/acsinfecdis.0c00675
ACS Infect. Dis. 2021, 7, 141−152

to 4 weeks. The MIC was defined as the lowest concentration of drug that prevented the growth of *Mtb*.

High Throughput Screening. The pilot screening was performed at GSK, Tres Cantos, Spain using exponentially growing WT and *mmpL3*-TetON as previously described in Middlebrook 7H9−ADN medium and flat bottom black/clear 384-well plates (Grenier Bio-One) containing 220 compounds of the GSK Tb-set dispensed via Echo acoustic liquid handler. The single cell suspensions were prepared by centrifuging the cultures at 800 rpm for 10 min. The resulting suspension of strains was diluted to an $OD_{580} \approx 0.01$ and dispensed onto the compound plates using the Multidrop dispenser (Thermo Fisher) followed by incubation at 37 °C, 5% CO_2 at 80% relative humidity for up to 10 days. Rifampicin at 1 μg/mL was used as positive control for inhibition and DMSO was maintained at 1%. The OD_{580} for two treatment groups were read using a SpectraMax M5 and the data was analyzed using Activity Base software to get primary hits. Subsequent confirmatory screenings were performed with shortlisted hits in a similar manner as described for drug susceptibility assays. The robustness of data was assessed by Z′ factor with a value of >0.8 as the cut off limit.

EchA6 Binding Assay. The recombinant protein, EchA6, was expressed and purified as previously described.[23] Briefly, *Escherichia coli* BL21 (DE3), harboring the pET28a-*echA6* vector, were grown in 1 L LB at 37 °C, 180 rpm, to OD_{600} of 0.4−0.6. Recombinant EchA6 expression was induced by the addition of 1 mM Isopropyl β-D-1-thiogalactopyranoside (IPTG), at 16 °C for 24 h. Following harvesting, the cell pellet was resuspended in 50 mM sodium phosphate, 600 mM sodium chloride and 10 mM imidazole (pH 8) containing a complete EDTA-free Protease Inhibitor Cocktail Tablet (Roche), and cells were sonicated on ice and then centrifuged at 27 000*g* (15 000 rpm) for 40 min. Recombinant EchA6 was purified from the supernatant using immobilized metal affinity chromatography (IMAC) by exploiting the vector-encoded poly histidine tag. The pure protein was subsequently dialyzed into 25 mM HEPES, 10% glycerol, and 300 mM NaCl (pH 8), and then concentrated.

Intrinsic tryptophan fluorescence was used to assay the binding of the compounds GSK1589673A, GSK1180781A, GSK1589671A, and GSK1941290A, and the control compounds GSK366A and GSK951A to the recombinant EchA6. Compounds were added at increasing stoichiometric ratios (GSK951A, 0.5−8 μM; GSK366A, 2−50 μM; GSK1589673A, GSK1180781A, and GSK1589671A, 0.5−20 μM; GSK1941290A, 2−100 μM to 3 μM EchA6 in 25 mM HEPES, 10% glycerol, and 300 mM NaCl (pH 8)). Fluorescence spectra were measured at 25 °C with an excitation wavelength of 280 nm (5 nm slit width) and emission wavelength of 300−400 nm (5 nm slit width), conducted on a Hitachi F7000 Fluorescence Spectrophotometer and recorded using Hitachi FL Solutions 4.6 software. Changes in fluorescence intensities due to increasing compound concentrations were corrected for. Data were analyzed in GraphPad Prism 6.

Membrane Potential Measurements in Intact Mtb. The effect of over- and under-expression of MmpL3 on transmembrane potential (ΔΨ) in intact bacilli was determined using fluorescence quenching of the ΔΨ-sensitive probe 3,3′-diethyloxacarbocyanine iodide ($DiOC_2(3)$) (Thermo Fisher). WT H37Rv and *mmpL3*-TetON were labeled with 50 μM $DiOC_2(3)$ in fresh 7H9−ADN for up to 30 min. Excess $DiOC_2(3)$ was washed off and an equal volume of bacteria at an OD_{580} of 0.8 were then aliquoted in black 96-well plates (clear bottom) for reading. Samples were also treated with 500 μM carbonyl cyanide *m*-chlorophenyl hydrazone (CCCP, positive control). The change in fluorescence due to disruption of ΔΨ was monitored with a fluorescence spectrophotometer (Spectramax M2e). $DiOC_2(3)$ was excited at 485 nm, and emission was measured at 615 and 535 nm. The red/green (610 nm/535 nm) fluorescence intensity ratio was calculated and used to quantify the strength of ΔΨ.

Ethidium Bromide Uptake Assay in Microtiter Plates. Strains were grown to OD_{580} of 0.8−1.0 as described above. Cells were washed once and resuspended in PBS supplemented with 0.02% tyloxapol and adjusted to an OD_{580} of 0.8. Glucose was then added to a final concentration of 0.8% to trigger metabolism and cells were distributed at 100 μL per well in a black 96-well microtiter plate with clear bottoms. Subsequently, an equal volume of ethidium bromide in PBS supplemented with 0.02% tyloxapol and 0.8% glucose was added to a final concentration of 4 μg/mL. The kinetics of fluorescence was measured every minute for 60 min at 37 °C using a fluorescence spectrophotometer (Spectramax M5, excitation at 530 nm, emission at 590 nm). Measurements were performed in triplicates.

Isolation of CCI7967-Resistant Mutants. *Mtb* H37Rv was grown to an OD_{580} of 0.8−1 to get a dense inoculum corresponding to approximately 10^9 bacteria. The culture was serially diluted and 100 μL of dilutions including undiluted, 10^{-1}, and 10^{-2} were cultured on 7H10 agar plates containing CCI7967 at a concentration of 4 × MIC. Lower dilutions were used to enumerate cell titer. Frequency of resistance was calculated as the number of resistant CFU thus obtained per 10^9 bacteria plated. Twelve resistant colonies were picked and inoculated in 5 mL of 7H9-ADN and grown to OD_{580} of 0.8. The level of resistance was assessed using antibiotic susceptibility assays as mentioned above. Four mutants were selected, purified genomic DNA was isolated using Epicenter MasterPure DNA/RNA isolation kit (Lucigen), sequenced, and analyzed for SNPs.

Chromosomal DNA Sequencing and Polymorphism Analysis. Between 150 and 200 ng of genomic DNA was sheared acoustically and HiSeq sequencing libraries were prepared using the KAPA Hyper Prep Kit (Roche). PCR amplification of the libraries was carried out for 10 cycles. (5−10) × 10^6 50-bp paired-end reads were obtained for each sample on an Illumina HiSeq 2500 using the TruSeq SBS Kit v3 (Illumina). Postrun demultiplexing and adapter removal were performed and fastq files were inspected using FastQC.[77] Trimmed fastq files were then aligned to the reference genome (*Mtb* H37RvCO; NZ_CM001515.1) using bwa mem.[74] Bam files were sorted and merged using SAM tools.[75] Read groups were added and bam files deduplicated using Picard tools and GATK best-practices were followed for SNP and indel detection.[76] The sequences thus assembled can be accessed through GenBank (NCBI) using the accession codes SAMN14986274 for WT (parent), and SAMN14986281 and SAMN14986282 for the mutants with SNPs in MmpL3.

Synergy Testing. Synergistic interactions were assessed in 384-well plates using the checkerboard assay format. Plates were dispensed using an HP D300e digital dispenser. The fractional inhibitory concentration (FIC) for each compound was calculated as follows: FIC_A = (MIC_{90} of compound A in the presence of compound B)/(MIC_{90} of compound A).

https://dx.doi.org/10.1021/acsinfecdis.0c00675
ACS Infect. Dis. 2021, 7, 141−152

Similarly, the FIC for compound B (FIC_B) was calculated. The FIC Index (FICI) was calculated as FICI = [FIC_A + FIC_B]. Synergy was defined by FICI values ≤0.5, antagonism by FICI values >4.0, and no interaction by FICI values from 0.5 to 4.0.

Quantification and Statistical Analysis. Graphic data were prepared with GraphPad Prism software and the results were analyzed as stated in the text. Two-tailed unpaired Student's *t* test was used for the analysis of differences between two groups. Statistical significance was defined as $P < 0.05$ unless otherwise stated.

Data Availability. Compound structures are available at ChEMBL (https://www.ebi.ac.uk/chembl/) and can be accessed using the doc ID CHEMBL2095176, previously published in Ballell, L. et al., 2013.[5]

■ ASSOCIATED CONTENT

Supporting Information

The Supporting Information is available free of charge at https://pubs.acs.org/doi/10.1021/acsinfecdis.0c00675.

> Susceptibility profile of under-expresser against drugs of known mechanism of action (Figure S1), large molecular weight antibiotics (Figure S2), structures of hits (Figure S3), binding of EchA6 to the THPPs as identified (Figure S4), scaffolds that do not interfere with *Mtb* ETC (Figure S5 and S6), scaffolds that interfere with *Mtb* ETC (Figure S7), susceptibility of *mmpL3*-TetON to hits (Table S1), cross-resistance of MmpL3 mutants against the compounds of unknown mechanism of action (Table S2), strains and plasmids (Table S3) (PDF)

■ AUTHOR INFORMATION

Corresponding Authors

Shipra Grover − *Department of Microbiology and Immunology, Weill Cornell Medicine, New York 10065, United States;* orcid.org/0000-0001-7094-6879; Email: shg2019@med.cornell.edu

Dirk Schnappinger − *Department of Microbiology and Immunology, Weill Cornell Medicine, New York 10065, United States*; Email: dis2003@med.cornell.edu

Authors

Curtis A. Engelhart − *Department of Microbiology and Immunology, Weill Cornell Medicine, New York 10065, United States*

Esther Pérez-Herrán − *TB Research Unit, Global Health R&D, GlaxoSmithKline, Madrid 28760, Spain*

Wei Li − *Mycobacteria Research Laboratories, Department of Microbiology, Immunology and Pathology, Colorado State University, Fort Collins, Colorado 80523, United States*

Katherine A. Abrahams − *Institute of Microbiology and Infection, School of Biological Sciences, University of Birmingham, Birmingham B15 2TT, U.K.*

Kadamba Papavinasasundaram − *Department of Microbiology and Physiological Systems, University of Massachusetts Medical School, Worcester, Massachusetts 01655, United States*

James M. Bean − *Sloan Kettering Institute, New York 10065, United States*

Christopher M. Sassetti − *Department of Microbiology and Physiological Systems, University of Massachusetts Medical School, Worcester, Massachusetts 01655, United States*

Alfonso Mendoza-Losana − *TB Research Unit, Global Health R&D, GlaxoSmithKline, Madrid 28760, Spain*

Gurdyal S. Besra − *Institute of Microbiology and Infection, School of Biological Sciences, University of Birmingham, Birmingham B15 2TT, U.K.;* orcid.org/0000-0002-5605-0395

Mary Jackson − *Mycobacteria Research Laboratories, Department of Microbiology, Immunology and Pathology, Colorado State University, Fort Collins, Colorado 80523, United States;* orcid.org/0000-0002-9212-0258

Complete contact information is available at: https://pubs.acs.org/10.1021/acsinfecdis.0c00675

Author Contributions

S.G., E.P.H., A.M.L., G.S.B., and D.S. conceived the study. E.P.H., W.L., and M.J. generated reagents. S.G., C.A.E., K.A.A., J.M.B., and K.P. conducted the experiments and performed data analysis. S.G., E.P.H., K.A.A., J.M.B., K.P., C.M.S., G.S.B., M.J., and D.S. wrote or contributed to the manuscript.

Notes

The authors declare no competing financial interest.

■ ACKNOWLEDGMENTS

We thank C. Alemparte, J. B. Wallach, and S. Song for technical support. We also acknowledge S. Ehrt and C. F. Nathan for their discussions and expertise in the field, and M. Glickman, L. Ballel, and D. Barros for access to infrastructure. We thank Scott A. Shaffer at the Proteomic and Mass Spectrometry Facility at the University of Massachusetts Medical School, for the MmpL3 Parallel Reaction Monitoring Assay. This research was supported by the Tres Cantos Open Lab Foundation (Project TC112), the Tri-Institutional TB Research Unit (NIH grant U19 AI111143), and the National Institute of Allergy and Infectious Diseases of the NIH (grant R01AI116525). G.S.B. acknowledges support in the form of a Personal Research Chair from Mr. James Bardrick and the Medical Research Council, UK (MR/R001154/1 and MR/S000542/1). We acknowledge the use of the Integrated Genomics Operation Core at MSKCC, funded by the NCI Cancer Center Support Grant (CCSG, P30 CA08748), Cycle for Survival and the Marie-Josée and Henry R. Kravis Center for Molecular Oncology.

■ ABBREVIATIONS

Mtb, *Mycobacterium tuberculosis*; *Mab*, *Mycobacterium abscessus*; TB, tuberculosis; WHO, World Health Organization; WCS, whole-cell screens; RND, resistance nodulation and division; TMM, trehalose mono mycolate; THPP, tetrahydropyrazolopyrimidines; Spiros, spirocycles; PMF, proton motive force; GSK, GlaxoSmithKline; TB-set, GlaxoSmithKline-Tres Cantos antimycobacterial set; ATc, anhydrotetracycline; ETC, electron transport chain; IPA, imidazopyridine amine; QoA, quinolone; TPA, thienopyrimidine amine; CCCP, carbocyanide *m*-chlorophenyl hydrazine, 3,3′-diethyloxacarbocyanine iodide; EtBr, ethidium bromide; IPTG, isopropyl β-D-1-thiogalactopyranoside; EchA6, enoyl coenzyme A hydratase; HTS, high throughput screen; SNPs, single nucleotide polymorphisms; OADC, oleic acid albumin dextrose catalase; ADN, albumin dextrose sodium chloride; IMAC, immobilized metal affinity chromatography; SE, standard error of the mean; FIC, fractional inhibitory concentration.

REFERENCES

(1) WHO. (2019) *Global Tuberculosis Report*, World Health Organization, Geneva, Switzerland.

(2) Pradipta, I. S., Forsman, L. D., Bruchfeld, J., Hak, E., and Alffenaar, J. W. (2018) Risk factors of multidrug-resistant tuberculosis: A global systematic review and meta-analysis. *J. Infect. 77*, 469−478.

(3) Imperial, M. Z., Nahid, P., Phillips, P. P. J., Davies, G. R., Fielding, K., Hanna, D., Hermann, D., Wallis, R. S., Johnson, J. L., Lienhardt, C., and Savic, R. M. (2018) A patient-level pooled analysis of treatment-shortening regimens for drug-susceptible pulmonary tuberculosis. *Nat. Med. 24*, 1708−1715.

(4) Sala, C., and Hartkoorn, R. C. (2011) Tuberculosis drugs: new candidates and how to find more. *Future Microbiol. 6*, 617−633.

(5) Ballell, L., Bates, R. H., Young, R. J., Alvarez-Gomez, D., Alvarez-Ruiz, E., Barroso, V., Blanco, D., Crespo, B., Escribano, J., Gonzalez, R., Lozano, S., Huss, S., Santos-Villarejo, A., Martin-Plaza, J. J., Mendoza, A., Rebollo-Lopez, M. J., Remuinan-Blanco, M., Lavandera, J. L., Perez-Herran, E., Gamo-Benito, F. J., Garcia-Bustos, J. F., Barros, D., Castro, J. P., and Cammack, N. (2013) Fueling open-source drug discovery: 177 small-molecule leads against tuberculosis. *ChemMedChem 8*, 313−321.

(6) Tahlan, K., Wilson, R., Kastrinsky, D. B., Arora, K., Nair, V., Fischer, E., Barnes, S. W., Walker, J. R., Alland, D., Barry, C. E., 3rd, and Boshoff, H. I. (2012) SQ109 targets MmpL3, a membrane transporter of trehalose monomycolate involved in mycolic acid donation to the cell wall core of *Mycobacterium tuberculosis*. *Antimicrob. Agents Chemother. 56*, 1797−1809.

(7) La Rosa, V., Poce, G., Canseco, J. O., Buroni, S., Pasca, M. R., Biava, M., Raju, R. M., Porretta, G. C., Alfonso, S., Battilocchio, C., Javid, B., Sorrentino, F., Ioerger, T. R., Sacchettini, J. C., Manetti, F., Botta, M., De Logu, A., Rubin, E. J., and De Rossi, E. (2012) MmpL3 is the cellular target of the antitubercular pyrrole derivative BM212. *Antimicrob. Agents Chemother. 56*, 324−331.

(8) Remuinan, M. J., Perez-Herran, E., Rullas, J., Alemparte, C., Martinez-Hoyos, M., Dow, D. J., Afari, J., Mehta, N., Esquivias, J., Jimenez, E., Ortega-Muro, F., Fraile-Gabaldon, M. T., Spivey, V. L., Loman, N. J., Pallen, M. J., Constantinidou, C., Minick, D. J., Cacho, M., Rebollo-Lopez, M. J., Gonzalez, C., Sousa, V., Angulo-Barturen, I., Mendoza-Losana, A., Barros, D., Besra, G. S., Ballell, L., and Cammack, N. (2013) Tetrahydropyrazolo[1,5-*a*]pyrimidine-3-carboxamide and *N*-benzyl-6′,7′-dihydrospiro[piperidine-4,4′-thieno[3,2-*c*]-pyran] analogues with bactericidal efficacy against *Mycobacterium tuberculosis* targeting MmpL3. *PLoS One 8*, e60933.

(9) Grzegorzewicz, A. E., Pham, H., Gundi, V. A., Scherman, M. S., North, E. J., Hess, T., Jones, V., Gruppo, V., Born, S. E., Kordulakova, J., Chavadi, S. S., Morisseau, C., Lenaerts, A. J., Lee, R. E., McNeil, M. R., and Jackson, M. (2012) Inhibition of mycolic acid transport across the *Mycobacterium tuberculosis* plasma membrane. *Nat. Chem. Biol. 8*, 334−341.

(10) Rao, S. P., Lakshminarayana, S. B., Kondreddi, R. R., Herve, M., Camacho, L. R., Bifani, P., Kalapala, S. K., Jiricek, J., Ma, N. L., Tan, B. H., Ng, S. H., Nanjundappa, M., Ravindran, S., Seah, P. G., Thayalan, P., Lim, S. H., Lee, B. H., Goh, A., Barnes, W. S., Chen, Z., Gagaring, K., Chatterjee, A. K., Pethe, K., Kuhen, K., Walker, J., Feng, G., Babu, S., Zhang, L., Blasco, F., Beer, D., Weaver, M., Dartois, V., Glynne, R., Dick, T., Smith, P. W., Diagana, T. T., and Manjunatha, U. H. (2013) Indolcarboxamide is a preclinical candidate for treating multidrug-resistant tuberculosis. *Sci. Transl. Med. 5*, 214ra168.

(11) Low, J. L., Wu, M. L., Aziz, D. B., Laleu, B., and Dick, T. (2017) Screening of TB actives for activity against nontuberculous mycobacteria delivers high hit rates. *Front. Microbiol. 8*, 1539.

(12) Tantry, S. J., Degiacomi, G., Sharma, S., Jena, L. K., Narayan, A., Guptha, S., Shanbhag, G., Menasinakai, S., Mallya, M., Awasthy, D., Balakrishnan, G., Kaur, P., Bhattacharjee, D., Narayan, C., Reddy, J., Naveen Kumar, C. N., Shandil, R., Boldrin, F., Ventura, M., Manganelli, R., Hartkoorn, R. C., Cole, S. T., Panda, M., Markad, S. D., Ramachandran, V., Ghorpade, S. R., and Dinesh, N. (2015) Whole cell screen based identification of spiropiperidines with potent antitubercular properties. *Bioorg. Med. Chem. Lett. 25*, 3234−3245.

(13) Lee, B. S., and Pethe, K. (2018) Therapeutic potential of promiscuous targets in *Mycobacterium tuberculosis*. *Curr. Opin. Pharmacol. 42*, 22−26.

(14) Zheng, H., Williams, J. T., Coulson, G. B., Haiderer, E. R., and Abramovitch, R. B. (2018) HC2091 kills *Mycobacterium tuberculosis* by targeting the MmpL3 mycolic acid transporter. *Antimicrob. Agents Chemother. 62*, e02459-17.

(15) Varela, C., Rittmann, D., Singh, A., Krumbach, K., Bhatt, K., Eggeling, L., Besra, G. S., and Bhatt, A. (2012) MmpL genes are associated with mycolic acid metabolism in mycobacteria and corynebacteria. *Chem. Biol. 19*, 498−506.

(16) Xu, Z., Meshcheryakov, V. A., Poce, G., and Chng, S. S. (2017) MmpL3 is the flippase for mycolic acids in mycobacteria. *Proc. Natl. Acad. Sci. U. S. A. 114*, 7993−7998.

(17) Yamaryo-Botte, Y., Rainczuk, A. K., Lea-Smith, D. J., Brammananth, R., van der Peet, P. L., Meikle, P., Ralton, J. E., Rupasinghe, T. W., Williams, S. J., Coppel, R. L., Crellin, P. K., and McConville, M. J. (2015) Acetylation of trehalose mycolates is required for efficient MmpL-mediated membrane transport in *Corynebacterineae*. *ACS Chem. Biol. 10*, 734−746.

(18) Degiacomi, G., Benjak, A., Madacki, J., Boldrin, F., Provvedi, R., Palu, G., Kordulakova, J., Cole, S. T., and Manganelli, R. (2017) Essentiality of mmpL3 and impact of its silencing on *Mycobacterium tuberculosis* gene expression. *Sci. Rep. 7*, 43495.

(19) Li, W., Obregon-Henao, A., Wallach, J. B., North, E. J., Lee, R. E., Gonzalez-Juarrero, M., Schnappinger, D., and Jackson, M. (2016) Therapeutic potential of the *Mycobacterium tuberculosis* mycolic acid transporter, MmpL3. *Antimicrob. Agents Chemother. 60*, 5198−5207.

(20) Lun, S., Guo, H., Onajole, O. K., Pieroni, M., Gunosewoyo, H., Chen, G., Tipparaju, S. K., Ammerman, N. C., Kozikowski, A. P., and Bishai, W. R. (2013) Indoleamides are active against drug-resistant *Mycobacterium tuberculosis*. *Nat. Commun. 4*, 2907.

(21) Ioerger, T. R., O'Malley, T., Liao, R., Guinn, K. M., Hickey, M. J., Mohaideen, N., Murphy, K. C., Boshoff, H. I., Mizrahi, V., Rubin, E. J., Sassetti, C. M., Barry, C. E., 3rd, Sherman, D. R., Parish, T., and Sacchettini, J. C. (2013) Identification of new drug targets and resistance mechanisms in *Mycobacterium tuberculosis*. *PLoS One 8*, e75245.

(22) Protopopova, M., Hanrahan, C., Nikonenko, B., Samala, R., Chen, P., Gearhart, J., Einck, L., and Nacy, C. A. (2005) Identification of a new antitubercular drug candidate, SQ109, from a combinatorial library of 1,2-ethylenediamines. *J. Antimicrob. Chemother. 56*, 968−974.

(23) Cox, J. A., Abrahams, K. A., Alemparte, C., Ghidelli-Disse, S., Rullas, J., Angulo-Barturen, I., Singh, A., Gurcha, S. S., Nataraj, V., Bethell, S., Remuinan, M. J., Encinas, L., Jervis, P. J., Cammack, N. C., Bhatt, A., Kruse, U., Bantscheff, M., Futterer, K., Barros, D., Ballell, L., Drewes, G., and Besra, G. S. (2016) THPP target assignment reveals EchA6 as an essential fatty acid shuttle in mycobacteria. *Nat. Microbiol 1*, 15006.

(24) Poce, G., Bates, R. H., Alfonso, S., Cocozza, M., Porretta, G. C., Ballell, L., Rullas, J., Ortega, F., De Logu, A., Agus, E., La Rosa, V., Pasca, M. R., De Rossi, E., Wae, B., Franzblau, S. G., Manetti, F., Botta, M., and Biava, M. (2013) Improved BM212 MmpL3 inhibitor analogue shows efficacy in acute murine model of tuberculosis infection. *PLoS One 8*, e56980.

(25) Li, K., Schurig-Briccio, L. A., Feng, X., Upadhyay, A., Pujari, V., Lechartier, B., Fontes, F. L., Yang, H., Rao, G., Zhu, W., Gulati, A., No, J. H., Cintra, G., Bogue, S., Liu, Y. L., Molohon, K., Orlean, P., Mitchell, D. A., Freitas-Junior, L., Ren, F., Sun, H., Jiang, T., Li, Y., Guo, R. T., Cole, S. T., Gennis, R. B., Crick, D. C., and Oldfield, E. (2014) Multitarget drug discovery for tuberculosis and other infectious diseases. *J. Med. Chem. 57*, 3126−3139.

(26) Sacksteder, K. A., Protopopova, M., Barry, C. E., 3rd, Andries, K., and Nacy, C. A. (2012) Discovery and development of SQ109: a new antitubercular drug with a novel mechanism of action. *Future Microbiol. 7*, 823−837.

https://dx.doi.org/10.1021/acsinfecdis.0c00675
ACS Infect. Dis. 2021, 7, 141−152

(27) Li, W., Sanchez-Hidalgo, A., Jones, V., de Moura, V. C., North, E. J., and Jackson, M. (2017) Synergistic interactions of MmpL3 inhibitors with antitubercular compounds *in vitro*. *Antimicrob. Agents Chemother.*, DOI: 10.1128/AAC.02399-16.
(28) Chen, P., Gearhart, J., Protopopova, M., Einck, L., and Nacy, C. A. (2006) Synergistic interactions of SQ109, a new ethylene diamine, with front-line antitubercular drugs in vitro. *J. Antimicrob. Chemother. 58*, 332−337.
(29) Stec, J., Onajole, O. K., Lun, S., Guo, H., Merenbloom, B., Vistoli, G., Bishai, W. R., and Kozikowski, A. P. (2016) Indole-2-carboxamide-based MmpL3 inhibitors show exceptional antitubercular activity in an animal model of tuberculosis infection. *J. Med. Chem. 59*, 6232−6247.
(30) WHO. (2018) *Global Tuberculosis Report*, World Health Organization, Geneva, Switzerland.
(31) Boeree, M. J., Heinrich, N., Aarnoutse, R., Diacon, A. H., Dawson, R., Rehal, S., Kibiki, G. S., Churchyard, G., Sanne, I., Ntinginya, N. E., Minja, L. T., Hunt, R. D., Charalambous, S., Hanekom, M., Semvua, H. H., Mpagama, S. G., Manyama, C., Mtafya, B., Reither, K., Wallis, R. S., Venter, A., Narunsky, K., Mekota, A., Henne, S., Colbers, A., van Balen, G. P., Gillespie, S. H., Phillips, P. P. J., Hoelscher, M., and Pan, A. c. (2017) High-dose rifampicin, moxifloxacin, and SQ109 for treating tuberculosis: a multi-arm, multi-stage randomised controlled trial. *Lancet Infect. Dis. 17*, 39−49.
(32) Williams, J. T., Haiderer, E. R., Coulson, G. B., Conner, K. N., Ellsworth, E., Chen, C., Alvarez-Cabrera, N., Li, W., Jackson, M., Dick, T., and Abramovitch, R. B. (2019) Identification of new MmpL3 inhibitors by untargeted and targeted mutant screens defines MmpL3 domains with differential resistance. *Antimicrob. Agents Chemother.*, DOI: 10.1128/AAC.00547-19.
(33) Li, W., Upadhyay, A., Fontes, F. L., North, E. J., Wang, Y., Crans, D. C., Grzegorzewicz, A. E., Jones, V., Franzblau, S. G., Lee, R. E., Crick, D. C., and Jackson, M. (2014) Novel insights into the mechanism of inhibition of MmpL3, a target of multiple pharmacophores in *Mycobacterium tuberculosis*. *Antimicrob. Agents Chemother. 58*, 6413−6423.
(34) Li, W., Stevens, C. M., Pandya, A. N., Darzynkiewicz, Z., Bhattarai, P., Tong, W., Gonzalez-Juarrero, M., North, E. J., Zgurskaya, H. I., and Jackson, M. (2019) Direct inhibition of MmpL3 by novel antitubercular compounds. *ACS Infect. Dis. 5*, 1001−1012.
(35) Zhang, B., Li, J., Yang, X., Wu, L., Zhang, J., Yang, Y., Zhao, Y., Zhang, L., Yang, X., Yang, X., Cheng, X., Liu, Z., Jiang, B., Jiang, H., Guddat, L. W., Yang, H., and Rao, Z. (2019) Crystal structures of membrane transporter MmpL3, an anti-TB drug target. *Cell 176*, 636−648.
(36) Lin, K., O'Brien, K. M., Trujillo, C., Wang, R., Wallach, J. B., Schnappinger, D., and Ehrt, S. (2016) *Mycobacterium tuberculosis* thioredoxin reductase is essential for thiol redox homeostasis but plays a minor role in antioxidant defense. *PLoS Pathog. 12*, e1005675.
(37) Manganelli, R., Voskuil, M. I., Schoolnik, G. K., Dubnau, E., Gomez, M., and Smith, I. (2002) Role of the extracytoplasmic-function sigma factor sigma(H) in *Mycobacterium tuberculosis* global gene expression. *Mol. Microbiol. 45*, 365−374.
(38) Belardinelli, J. M., Yazidi, A., Yang, L., Fabre, L., Li, W., Jacques, B., Angala, S. K., Rouiller, I., Zgurskaya, H. I., Sygusch, J., and Jackson, M. (2016) Structure-function profile of MmpL3, the essential mycolic acid transporter from *Mycobacterium tuberculosis*. *ACS Infect. Dis. 2*, 702−713.
(39) Pal, R., Hameed, S., and Fatima, Z. (2019) Altered drug efflux under iron deprivation unveils abrogated MmpL3 driven mycolic acid transport and fluidity in mycobacteria. *BioMetals 32*, 49−63.
(40) Jackson, M., Raynaud, C., Laneelle, M. A., Guilhot, C., Laurent-Winter, C., Ensergueix, D., Gicquel, B., and Daffe, M. (1999) Inactivation of the antigen 85C gene profoundly affects the mycolate content and alters the permeability of the *Mycobacterium tuberculosis* cell envelope. *Mol. Microbiol. 31*, 1573−1587.
(41) Rodrigues, L., Viveiros, M., and Ainsa, J. A. (2015) Measuring efflux and permeability in mycobacteria. *Methods Mol. Biol. 1285*, 227−239.
(42) Rebollo-Lopez, M. J., Lelievre, J., Alvarez-Gomez, D., Castro-Pichel, J., Martinez-Jimenez, F., Papadatos, G., Kumar, V., Colmenarejo, G., Mugumbate, G., Hurle, M., Barroso, V., Young, R. J., Martinez-Hoyos, M., Gonzalez del Rio, R., Bates, R. H., Lopez-Roman, E. M., Mendoza-Losana, A., Brown, J. R., Alvarez-Ruiz, E., Marti-Renom, M. A., Overington, J. P., Cammack, N., Ballell, L., and Barros-Aguire, D. (2015) Release of 50 new, drug-like compounds and their computational target predictions for open source anti-tubercular drug discovery. *PLoS One 10*, No. e0142293.
(43) Trofimov, V., Kicka, S., Mucaria, S., Hanna, N., Ramon-Olayo, F., Del Peral, L. V., Lelievre, J., Ballell, L., Scapozza, L., Besra, G. S., Cox, J. A. G., and Soldati, T. (2018) Antimycobacterial drug discovery using Mycobacteria-infected amoebae identifies anti-infectives and new molecular targets. *Sci. Rep. 8*, 3939.
(44) Zampieri, M., Szappanos, B., Buchieri, M. V., Trauner, A., Piazza, I., Picotti, P., Gagneux, S., Borrell, S., Gicquel, B., Lelievre, J., Papp, B., and Sauer, U. (2018) High-throughput metabolomic analysis predicts mode of action of uncharacterized antimicrobial compounds. *Sci. Transl. Med. 10*, eaal3973.
(45) Dupont, C., Chen, Y., Xu, Z., Roquet-Baneres, F., Blaise, M., Witt, A. K., Dubar, F., Biot, C., Guerardel, Y., Maurer, F. P., Chng, S. S., and Kremer, L. (2019) A piperidinol-containing molecule is active against *Mycobacterium tuberculosis* by inhibiting the mycolic acid flippase activity of MmpL3. *J. Biol. Chem. 294*, 17512.
(46) Dupont, C., Viljoen, A., Dubar, F., Blaise, M., Bernut, A., Pawlik, A., Bouchier, C., Brosch, R., Guerardel, Y., Lelievre, J., Ballell, L., Herrmann, J. L., Biot, C., and Kremer, L. (2016) A new piperidinol derivative targeting mycolic acid transport in *Mycobacterium abscessus*. *Mol. Microbiol. 101*, 515−529.
(47) Su, C. C., Klenotic, P. A., Bolla, J. R., Purdy, G. E., Robinson, C. V., and Yu, E. W. (2019) MmpL3 is a lipid transporter that binds trehalose monomycolate and phosphatidylethanolamine. *Proc. Natl. Acad. Sci. U. S. A. 116*, 11241−11246.
(48) Novo, D., Perlmutter, N. G., Hunt, R. H., and Shapiro, H. M. (1999) Accurate flow cytometric membrane potential measurement in bacteria using diethyloxacarbocyanine and a ratiometric technique. *Cytometry 35*, 55−63.
(49) Pethe, K., Bifani, P., Jang, J., Kang, S., Park, S., Ahn, S., Jiricek, J., Jung, J., Jeon, H. K., Cechetto, J., Christophe, T., Lee, H., Kempf, M., Jackson, M., Lenaerts, A. J., Pham, H., Jones, V., Seo, M. J., Kim, Y. M., Seo, M., Seo, J. J., Park, D., Ko, Y., Choi, I., Kim, R., Kim, S. Y., Lim, S., Yim, S. A., Nam, J., Kang, H., Kwon, H., Oh, C. T., Cho, Y., Jang, Y., Kim, J., Chua, A., Tan, B. H., Nanjundappa, M. B., Rao, S. P., Barnes, W. S., Wintjens, R., Walker, J. R., Alonso, S., Lee, S., Kim, J., Oh, S., Oh, T., Nehrbass, U., Han, S. J., No, Z., Lee, J., Brodin, P., Cho, S. N., Nam, K., and Kim, J. (2013) Discovery of Q203, a potent clinical candidate for the treatment of tuberculosis. *Nat. Med. 19*, 1157−1160.
(50) Preiss, L., Langer, J. D., Yildiz, Ö., Eckhardt-Strelau, L., Guillemont, J. E., Koul, A., and Meier, T. (2015) Structure of the mycobacterial ATP synthase F_o rotor ring in complex with the anti-TB drug bedaquiline. *Sci. Adv. 1*, e1500106.
(51) Koul, A., Dendouga, N., Vergauwen, K., Molenberghs, B., Vranckx, L., Willebrords, R., Ristic, Z., Lill, H., Dorange, I., Guillemont, J., Bald, D., and Andries, K. (2007) Diarylquinolines target subunit *c* of mycobacterial ATP synthase. *Nat. Chem. Biol. 3*, 323−324.
(52) Abrahams, K. A., Cox, J. A., Spivey, V. L., Loman, N. J., Pallen, M. J., Constantinidou, C., Fernandez, R., Alemparte, C., Remuinan, M. J., Barros, D., Ballell, L., and Besra, G. S. (2012) Identification of novel imidazo[1,2-*a*]pyridine inhibitors targeting *M. tuberculosis* QcrB. *PLoS One 7*, e52951.
(53) Phummarin, N., Boshoff, H. I., Tsang, P. S., Dalton, J., Wiles, S., Barry, C. E., 3rd, and Copp, B. R. (2016) SAR and identification of 2-(quinolin-4-yloxy)acetamides as *Mycobacterium tuberculosis* cytochrome bc_1 inhibitors. *MedChemComm 7*, 2122−2127.

(54) Kalia, N. P., Hasenoehrl, E. J., Ab Rahman, N. B., Koh, V. H., Ang, M. L. T., Sajorda, D. R., Hards, K., Grüber, G., Alonso, S., Cook, G. M., Berney, M., and Pethe, K. (2017) Exploiting the synthetic lethality between terminal respiratory oxidases to kill. *Proc. Natl. Acad. Sci. U. S. A. 114*, 7426−7431.
(55) Beites, T., O'Brien, K., Tiwari, D., Engelhart, C. A., Walters, S., Andrews, J., Yang, H. J., Sutphen, M. L., Weiner, D. M., Dayao, E. K., Zimmerman, M., Prideaux, B., Desai, P. V., Masquelin, T., Via, L. E., Dartois, V., Boshoff, H. I., Barry, C. E., Ehrt, S., and Schnappinger, D. (2019) Plasticity of the *Mycobacterium tuberculosis* respiratory chain and its impact on tuberculosis drug development. *Nat. Commun. 10*, 4970.
(56) Johnson, E. O., LaVerriere, E., Office, E., Stanley, M., Meyer, E., Kawate, T., Gomez, J. E., Audette, R. E., Bandyopadhyay, N., Betancourt, N., Delano, K., Da Silva, I., Davis, J., Gallo, C., Gardner, M., Golas, A. J., Guinn, K. M., Kennedy, S., Korn, R., McConnell, J. A., Moss, C. E., Murphy, K. C., Nietupski, R. M., Papavinasasundaram, K. G., Pinkham, J. T., Pino, P. A., Proulx, M. K., Ruecker, N., Song, N., Thompson, M., Trujillo, C., Wakabayashi, S., Wallach, J. B., Watson, C., Ioerger, T. R., Lander, E. S., Hubbard, B. K., Serrano-Wu, M. H., Ehrt, S., Fitzgerald, M., Rubin, E. J., Sassetti, C. M., Schnappinger, D., and Hung, D. T. (2019) Large-scale chemical-genetics yields new *M. tuberculosis* inhibitor classes. *Nature 571*, 72−78.
(57) Abrahams, G. L., Kumar, A., Savvi, S., Hung, A. W., Wen, S., Abell, C., Barry, C. E., 3rd, Sherman, D. R., Boshoff, H. I., and Mizrahi, V. (2012) Pathway-selective sensitization of *Mycobacterium tuberculosis* for target-based whole-cell screening. *Chem. Biol. 19*, 844−854.
(58) Schnappinger, D. (2015) Genetic approaches to facilitate antibacterial drug development. *Cold Spring Harbor Perspect. Med. 5*, a021139.
(59) Esposito, M., Szadocka, S., Degiacomi, G., Orena, B. S., Mori, G., Piano, V., Boldrin, F., Zemanová, J., Huszár, S., Barros, D., Ekins, S., Lelièvre, J., Manganelli, R., Mattevi, A., Pasca, M. R., Riccardi, G., Ballell, L., Mikušová, K., and Chiarelli, L. R. (2017) A phenotypic based target screening approach delivers new antitubercular CTP synthetase inhibitors. *ACS Infect. Dis. 3*, 428−437.
(60) Chiarelli, L. R., Mori, G., Orena, B. S., Esposito, M., Lane, T., de Jesus Lopes Ribeiro, A. L., Degiacomi, G., Zemanova, J., Szadocka, S., Huszar, S., Palcekova, Z., Manfredi, M., Gosetti, F., Lelievre, J., Ballell, L., Kazakova, E., Makarov, V., Marengo, E., Mikusova, K., Cole, S. T., Riccardi, G., Ekins, S., and Pasca, M. R. (2018) A multitarget approach to drug discovery inhibiting *Mycobacterium tuberculosis* PyrG and PanK. *Sci. Rep. 8*, 3187.
(61) Foo, C. S., Lupien, A., Kienle, M., Vocat, A., Benjak, A., Sommer, R., Lamprecht, D. A., Steyn, A. J. C., Pethe, K., Piton, J., Altmann, K. H., and Cole, S. T. (2018) Arylvinylpiperazine amides, a new class of potent inhibitors targeting QcrB of *Mycobacterium tuberculosis*. *mBio*, DOI: 10.1128/mBio.01276-18.
(62) Pandya, A. N., Prathipati, P. K., Hegde, P., Li, W., Graham, K. F., Mandal, S., Drescher, K. M., Destache, C. J., Ordway, D., Jackson, M., and North, E. J. (2019) Indole-2-carboxamides are active against *Mycobacterium abscessus* in a mouse model of acute infection. *Antimicrob. Agents Chemother.*, DOI: 10.1128/AAC.02245-18.
(63) Franz, N. D., Belardinelli, J. M., Kaminski, M. A., Dunn, L. C., Calado Nogueira de Moura, V., Blaha, M. A., Truong, D. D., Li, W., Jackson, M., and North, E. J. (2017) Design, synthesis and evaluation of indole-2-carboxamides with pan anti-mycobacterial activity. *Bioorg. Med. Chem. 25*, 3746−3755.
(64) De Groote, M. A., Jarvis, T. C., Wong, C., Graham, J., Hoang, T., Young, C. L., Ribble, W., Day, J., Li, W., Jackson, M., Gonzalez-Juarrero, M., Sun, X., and Ochsner, U. A. (2018) Optimization and lead selection of benzothiazole amide analogs toward a novel antimycobacterial agent. *Front. Microbiol. 9*, 2231.
(65) de Ruyck, J., Dupont, C., Lamy, E., Le Moigne, V., Biot, C., Guerardel, Y., Herrmann, J. L., Blaise, M., Grassin-Delyle, S., Kremer, L., and Dubar, F. (2020) Structure-based design and synthesis of piperidinol-containing molecules as new *Mycobacterium abscessus* inhibitors. *ChemistryOpen 9*, 351−365.
(66) Raynaud, C., Daher, W., Johansen, M. D., Roquet-Baneres, F., Blaise, M., Onajole, O. K., Kozikowski, A. P., Herrmann, J. L., Dziadek, J., Gobis, K., and Kremer, L. (2020) Active benzimidazole derivatives targeting the MmpL3 transporter in *Mycobacterium abscessus*. *ACS Infect. Dis. 6*, 324−337.
(67) Shetty, A., Xu, Z., Lakshmanan, U., Hill, J., Choong, M. L., Chng, S. S., Yamada, Y., Poulsen, A., Dick, T., and Gengenbacher, M. (2018) Novel acetamide indirectly targets mycobacterial transporter MmpL3 by proton motive force disruption. *Front. Microbiol. 9*, 2960.
(68) Kozikowski, A. P., Onajole, O. K., Stec, J., Dupont, C., Viljoen, A., Richard, M., Chaira, T., Lun, S., Bishai, W., Raj, V. S., Ordway, D., and Kremer, L. (2017) Targeting mycolic acid transport by indole-2-carboxamides for the treatment of *Mycobacterium abscessus* infections. *J. Med. Chem. 60*, 5876−5888.
(69) Li, W., Yazidi, A., Pandya, A. N., Hegde, P., Tong, W., Calado Nogueira de Moura, V., North, E. J., Sygusch, J., and Jackson, M. (2018) MmpL3 as a target for the treatment of drug-resistant nontuberculous mycobacterial infections. *Front. Microbiol. 9*, 1547.
(70) Brown-Elliott, B. A., Nash, K. A., and Wallace, R. J., Jr. (2012) Antimicrobial susceptibility testing, drug resistance mechanisms, and therapy of infections with nontuberculous mycobacteria. *Clin Microbiol Rev. 25*, 545−582.
(71) Nessar, R., Cambau, E., Reyrat, J. M., Murray, A., and Gicquel, B. (2012) *Mycobacterium abscessus*: a new antibiotic nightmare. *J. Antimicrob. Chemother. 67*, 810−818.
(72) Prigozhin, D. M., Papavinasasundaram, K. G., Baer, C. E., Murphy, K. C., Moskaleva, A., Chen, T. Y., Alber, T., and Sassetti, C. M. (2016) Structural and genetic analyses of the *Mycobacterium tuberculosis* Protein Kinase B sensor domain identify a potential ligand-binding site. *J. Biol. Chem. 291*, 22961−22969.
(73) Shin, A., Shin, B., Shin, J. W., Kim, K. H., Atwal, R. S., Hope, J. M., Gillis, T., Leszyk, J. D., Shaffer, S. A., Lee, R., Kwak, S., MacDonald, M. E., Gusella, J. F., Seong, I. S., and Lee, J. M. (2017) Novel allele-specific quantification methods reveal no effects of adult onset CAG repeats on HTT mRNA and protein levels. *Hum. Mol. Genet. 26*, 1258−1267.
(74) Li, H., and Durbin, R. (2009) Fast and accurate short read alignment with Burrows-Wheeler transform. *Bioinformatics 25*, 1754−1760.
(75) Li, H., Handsaker, B., Wysoker, A., Fennell, T., Ruan, J., Homer, N., Marth, G., Abecasis, G., and Durbin, R. (2009) The Sequence Alignment/Map format and SAMtools. *Bioinformatics 25*, 2078−2079.
(76) DePristo, M. A., Banks, E., Poplin, R., Garimella, K. V., Maguire, J. R., Hartl, C., Philippakis, A. A., del Angel, G., Rivas, M. A., Hanna, M., McKenna, A., Fennell, T. J., Kernytsky, A. M., Sivachenko, A. Y., Cibulskis, K., Gabriel, S. B., Altshuler, D., and Daly, M. J. (2011) A framework for variation discovery and genotyping using next-generation DNA sequencing data. *Nat. Genet. 43*, 491−498.
(77) Andrews, S. (2010) *FastQC: A Quality Control Tool for High Throughput Sequence Data*. http://www.bioinformatics.babraham.ac.uk/projects/fastqc.